

S. Kim Ratanathanawongs  
Williams  
Dean Lee

Department of Chemistry and  
Geochemistry, Colorado School  
of Mines, Golden, CO, USA

## Review

# Field-flow fractionation of proteins, polysaccharides, synthetic polymers, and supramolecular assemblies

This review summarizes developments and applications of flow and thermal field-flow fractionation (FFF) in the areas of macromolecules and supramolecular assemblies. In the past 10 years, the use of these FFF techniques has extended beyond determining diffusion coefficients, hydrodynamic diameters, and molecular weights of standards. Complex samples as diverse as polysaccharides, prion particles, and block copolymers have been characterized and processes such as aggregation, stability, and infectivity have been monitored. The open channel design used in FFF makes it a gentle separation technique for high- and ultrahigh-molecular weight macromolecules, aggregates, and self-assembled complexes. Coupling FFF with other techniques such as multiangle light scattering and MS provides additional invaluable information about conformation, branching, and identity.

**Keywords:** Nanomaterials / Polymers / Proteins / Protein aggregates / Supramolecular assemblies

Received: April 18, 2006; revised: May 9, 2006; accepted: May 9, 2006

DOI 10.1002/jssc.200600151

## 1 Introduction

Growth and development in fields such as nanomaterials and biotechnology have challenged existing analytical techniques in a myriad of new and different fronts. These samples are often complex with a wide distribution in molecular weight (MW), size, shape, charge, density, chemical composition, degree of branching, or microstructure (to name a few). Information about each of these distributions is used to determine their effect on materials properties or to verify products of new synthetic routes. In the biological field, the presence of protein aggregates is sometimes desirable and at other times not [1–3]. Analytical techniques have to be able to cope with samples that possess a high degree of heterogeneity and sizes that may reach upwards of several micrometers. A separation step is often necessary to produce fractions that are more

readily analyzed by light scattering, microscopy, MS, NMR, *etc.* Separation techniques capable of handling sample mixtures with large (micron-size) components include sieving, disk centrifugation [4], CE [5], capillary hydrodynamic fractionation [6], and the family of field-flow fractionation (FFF) techniques [7, 8].

FFF was introduced in 1966 as a method for separating larger sample species such as macromolecules, colloids, and particles [9]. The open channel design (devoid of packing material) lends itself to separations of particulate materials and shear sensitive samples. The FFF separation mechanism does not rely on adsorption or partitioning making this technique less likely to suffer sample loss. In the 40 years since its inception, FFF has been used in numerous applications including the separation of nanotubes [10, 11], stem and cancer cells [12, 13], pathogenic microorganisms [14–17], parasites [18–20], inorganic and polymeric particles [21, 22] and the study of processes such as cell apoptosis [23], surface adsorption [24–26], and hydrodynamic forces [27]. Two textbooks have been dedicated to FFF [28, 29] and review articles continue to be published addressing polymers [30, 31], proteins [32, 33], biotechnology [34], and particles (to be published, *Encyclopedia of Particle Technology* <http://nanoparticles.org/encyclopedia/>). The range of possible applications for FFF is enormous.

**Correspondence:** Professor S. Kim Ratanathanawongs Williams, Department of Chemistry and Geochemistry, Colorado School of Mines, Golden, CO 80401, USA.  
**E-mail:** krwillia@mines.edu.  
**Fax:** +1-303-273-3629.

**Abbreviations:** AG, arabinogalactan; AGP, AG-protein complex; AMP, amylopectin; AMY, amylose; EHEC, ethylhydroxylethyl cellulose; FFF, field-flow fractionation; FFFF, flow FFF; MALS-dRI, multiangle light scattering-differential refractive index; MW, molecular weight; rms, root mean square radius; SEC, size exclusion chromatography; ThFFF, thermal FFF

## 2 Separation mechanism and implementation

FFF is an elution-based separation technique that is implemented in an open rectangular channel as shown in Fig. 1. Under laminar flow conditions, the flow velocity across the channel thickness  $w$  has a parabolic profile with the highest flow velocity at the center of the channel and slowest velocity at the walls. An external field that is applied perpendicular to the separation axis interacts to different extents with different sample components. This field-induced transport toward the FFF channel wall (so-called accumulation wall) is balanced by a diffusion away from the wall. At equilibrium, a steady state is established for each sample component at a unique distance from the channel wall. The mean thickness of this sample equilibrium layer is related to the retention time and physicochemical properties of the sample. A sample component that interacts more strongly with the applied field and/or has a lower diffusion coefficient, e.g., sample component B, will establish a steady state closer to the accumulation wall and will have a longer retention time than component C.

Different FFF techniques arise as a result of different fields being applied. Sedimentation FFF uses a centrifugal field and is a high-resolution separation technique for submicrometer- to micrometer-sized particles [35]. However, its use for macromolecular analyses is limited because current commercially available systems do not provide sufficient field strength to induce retention of these relatively low mass analytes. Electrical FFF has

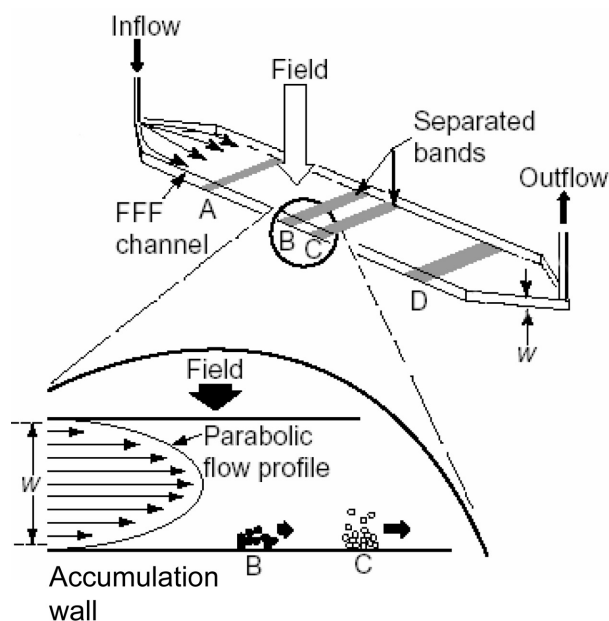


**Figure 1.** FFF separation mechanism. (Reprinted with permission from [31]; Copyright 2000 John Wiley & Sons.)

been applied to proteins [36], DNA [37], and polystyrene sulfonates [38], but has not been widely used because it is not commercially available. This review focuses on the most commonly used FFF techniques, crossflow and thermal FFF (ThFFF), and their application to macromolecules and supramolecular assemblies in the last 10 years.

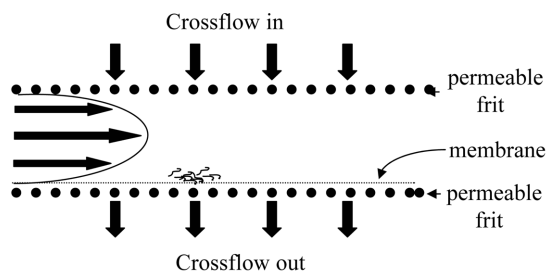
### 2.1 Crossflow FFF

Crossflow or flow FFF (FIFFF) utilizes a second fluid flow to transport sample components across the channel thickness to the accumulation wall [28, 29]. The entire sample is displaced regardless of mass, density, size, charge, etc. As a consequence, FIFFF is the most universally applicable FFF technique with applications encompassing macromolecules with MW of  $10^3$ – $10^9$  Da and particles 50  $\mu\text{m}$  in diameter [39]. For materials smaller than  $\sim 1 \mu\text{m}$ , separation occurs in the normal mode and the retention time is inversely proportional to diffusion coefficient  $D$  and proportional to the hydrodynamic diameter. The order of sample elution for the normal mode of operation is high diffusion coefficient (small particles or low MW macromolecules) followed by decreasing  $D$  (large particles or high MW macromolecules).

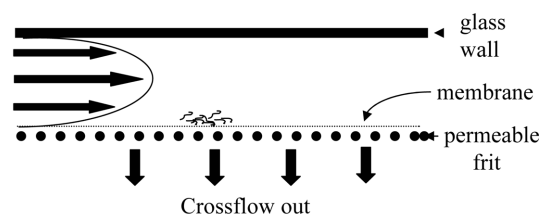
FIFFF is performed in rectangular channels in both symmetric and asymmetric configurations (Fig. 2a and b). Symmetric FIFFF, which is the original configuration, utilizes two permeable walls with the crossflow passing through both channel walls. Asymmetric FIFFF was introduced in 1987 [40] and has one permeable wall and one solid transparent wall. Despite more complicated theoretical equations, asymmetric FIFFF has become the more commonly used configuration because the transparent wall allows a visual performance check of the channel, higher efficiency has been observed [41, 42], and more companies offer this design. FIFFF systems are available through PostNova Analytics ([www.postnova.com](http://www.postnova.com)), ConSensus ([www.consensus.com](http://www.consensus.com)), and Wyatt Technologies ([www.wyatt.com](http://www.wyatt.com)). A third configuration that is not commercially available uses a cylindrical tube such as a hollow fiber (HF) membrane [43–45] or a ceramic HF [46] (Fig. 2c). The field, in this case, is radial with the crossflow radiating outwards over the entire internal surface of the tube while the channel flow moves down the length of the tube.

FIFFF has undergone a number of technical developments to facilitate its use for macromolecular and particulate analyses. Frit-inlet FIFFF was introduced as a means to quickly relax sample components to their different equilibrium distances above the accumulation wall [47]. Frit-outlet FIFFF was developed for on-line concentration prior to detection [47]. This feature addresses the dilute nature of many biological samples and compensates for some of the dilution that occurs during the separation process. These approaches have only been

### a. Symmetric flow FFF (rectangular channel)



### b. Asymmetric flow FFF (rectangular channel)



### c. Hollow fiber flow FFF (capillary tube)

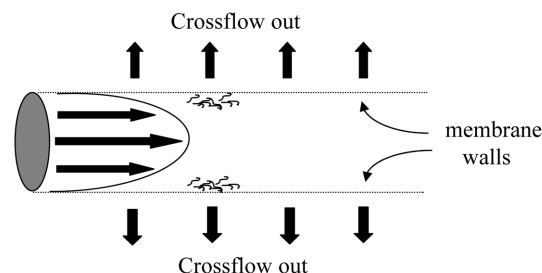


**Figure 2.** Different variants of FIFFF. (a) Symmetric FIFFF refers to a rectangular channel geometry with two permeable walls and was the original FIFFF configuration, (b) asymmetric FIFFF is also used in a rectangular channel geometry but has only one permeable wall, and (c) HF FIFFF is performed using a HF membrane or ceramic tube. (Reprinted with permission from [31]; Copyright 2000 John Wiley & Sons.)

demonstrated in symmetric FIFFF channels, but the concepts could also be realized in asymmetric channels.

Diffusion coefficients and hydrodynamic diameters can be calculated from measured retention times using existing theoretical FIFFF equations [28]. However, MW and MW distributions require the use of calibration standards [48] or a detector capable of measuring MW of the eluting sample. The most commonly used FIFFF detector is the UV detector which suffices for many applications. In the absence of MW calibration standards, the multiangle light scattering-differential refractometer (MALS-dRI) detector combination is used to measure MWs and root mean square radii ( $r_{ms}$ ) of the eluting samples [49]. The MALS-dRI detectors offer a simplification of the FIFFF

data analysis process. Slight nonidealities that affect retention volumes are not critically important as the MWs are measured by MALS. However, it is important to note that the separations aspect cannot be completely ignored, as low polydispersity samples are required for accurate MALS measurements. In addition, when analyzing large polymers (comparable to the size of the laser wavelength), MALS data analysis and interpretation have to be done carefully. A systematic study of the error estimation is available for different fitting approaches [50].

## 2.2 ThFFF

ThFFF has been used mainly for separations of organosoluble polymers [30] and to a lesser extent separations of particles [51, 52]. The “field” used in ThFFF is a temperature gradient (Fig. 3). One wall is heated using computer-controlled heating rods and the other wall is maintained at a lower temperature using a recirculating chiller [53]. The temperature gradient, arising from the temperature difference between a hot and a cold wall,  $\Delta T$ , causes thermal diffusion of sample toward the accumulation wall (usually cold wall). The retention time in ThFFF is proportional to  $\Delta T$  multiplied by the ratio of the thermal diffusion coefficient  $D_T$  to that of the normal diffusion coefficient. For homopolymers, sample species with higher  $D$  (or lower polymer MW) values elute first. The thermal diffusion process, on the other hand, is not sufficiently understood to be used for calculating retention times. Despite numerous empirical studies and proposed theories [54–58], thermal diffusion remains an intriguing, but highly useful, aspect of ThFFF separations. Composition-based separations have been demonstrated for both polymers [59–61] and particles [62]. This topic is discussed further in a later section.

As it is not possible to accurately predict  $D_T$ , ThFFF requires MW calibration standards or use with detectors that measure MW of the eluting components. Coupling FFF with MALS-dRI and MALDI-TOF-MS has proven to be mutually beneficial as these latter techniques require a certain degree of monodispersity and chemical homogeneity in the sample [60, 63]. Other detectors that have been used with ThFFF include refractive index and evaporative light scattering.

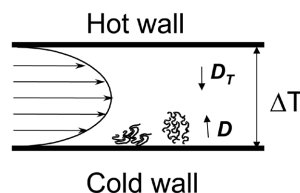


**Figure 3.** Schematic of thermal FF channel and separation mechanism. Thermal diffusion causes polymer migration towards the accumulation wall while diffusion transports polymers away from the wall.

In recent years, miniaturized ThFFF channels have been fabricated and used to separate synthetic polymers and particles [64–67]. Conventional ThFFF systems are offered by PostNova Analytics and the micro-ThFFF system is available through Watrex (www.watrex.cz).

### 3 FFF studies of macromolecules and supramolecular assemblies

Macromolecules of biological and synthetic origins have been analyzed by FIFFF and ThFFF. The open channel design makes FFF a gentle separation technique for high and ultrahigh MW macromolecules ( $10^{10}$  Da), environment-sensitive samples such as protein aggregates and ribosomes, and supramolecular assemblies such as liposomes and lipid–DNA complexes.

#### 3.1 Proteins, protein aggregates, and DNA

The capability of FIFFF to separate proteins was first demonstrated by Giddings in 1977 [68]. FIFFF was subsequently used to separate additional proteins [2], wheat proteins, monitor lipoprotein particle size distributions for potential use as a biomarker for the coronary artery disease [69], and investigate protein and DNA (linear and circular) conformation [70, 71]. These earlier studies were conducted with on-line UV detectors and relied upon developed FFF theory or calibration curves for transformation of the time-based fractograms into size or MW distributions.

In recent years, FIFFF has been coupled to other detectors, most notably, multiangle light scattering and differential refractive index or MALS-dRI. The combination has proven to be mutually beneficial as the FIFFF provides the essential “monodisperse” samples for MALS measurements and MALS eliminates the need for MW standards. In the separation of polymeric wheat proteins [72–74], the fractogram showed a tailing peak. The MALS detector determined that the molar mass of the component eluting at peak maximum was  $\sim 22\,500\text{--}300\,000$  Da, whereas the components eluting in the tail were near  $10\,000\,000$  Da [74]. The *rms* determined by MALS increased from 20 to 40 nm across the fractogram. The dramatic increase in MW compared to that in size suggested that the high-molar mass components eluting in the tail had a more compact conformation.

The separation of polymer wheat proteins by FIFFF demonstrated the suitability of the technique for analysis of ultrahigh MW species, which were beyond the limit of size exclusion chromatography (SEC). The open FFF channel results in low shear rates and gentle separations and would also prove to be ideally suited for separating protein aggregates. Asymmetric FIFFF was recently applied to a study that correlated the size of prion particles with infectivity. In this work, protease-resistant PrP

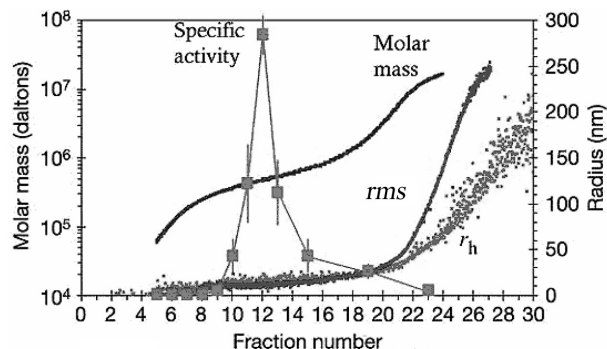


**Figure 4.** Analysis of fractionated PrP<sup>res</sup>, a protease-resistant form of the PRP protein. MALS-derived molar masses, root mean square radii, hydrodynamic radius, and specific infectivity are plotted for each fraction collected after separation by FIFFF. (Modified and reprinted with permission from [75]; Copyright 2005 Nature Publishing Group.)

protein (PrP<sup>res</sup>) aggregates were fractionated and molar mass, *rms*, and hydrodynamic radius ( $r_h$ ) were determined using on-line MALS and quasielastic light scattering (QELS) [75]. As shown in Fig. 4, the PrP<sup>res</sup> aggregates covered an *rms* range from  $<10$  to 250 nm and an  $r_h$  range of 5–200 nm. The molar mass was from  $6 \times 10^4$  to  $1 \times 10^7$  Da. The ratio of *rms*/ $r_h$  is an indicator of the shape of the aggregates. The ratios for the early fractions (8–19) were about 0.9, which indicated a spherical or ellipsoid shape. The ratios for the late fractions were higher than 1, suggestive of a more extended shape such as a fibril. The light scattering results were consistent with transmission electron microscopy images. Figure 4 also shows the specific infectivity of the PrP<sup>res</sup> aggregates from fractions 5 to 23. The infectivity peaked at fraction 12, which corresponded to the aggregates with molar mass, *rms*,  $r_h$  at  $5.35 \times 10^5$  Da, 12 nm, and 13 nm, respectively. The high specific infectivity of the small size aggregates suggested that the efforts to disaggregate amyloid fibrils in infected tissues may not be the right treatment approach as the most infectious prion particles may become dislodged.

The specific infectivity measurement of the fractionated PrP<sup>res</sup> aggregates demonstrated an important characteristic of FIFFF: a “gentle” separation method with the capability to maintain the biological activity of the analytes. HF FIFFF was used to study two grades of urate oxidase (uricase): a recombinant uricase drug from *Aspergillus flavus* expressed in *Saccharomyces cerevisiae* (termed Rasburicase) and a reagent-grade uricase from *Candida sphaerica* expressed in *Escherichia coli* (termed Sigma uricase) [76]. The fractogram of Rasburicase showed a single peak with the retention volume corresponding to the tetramer form of the protein. The fractogram of Sigma uricase showed a bimodal peak with the retention volumes cor-

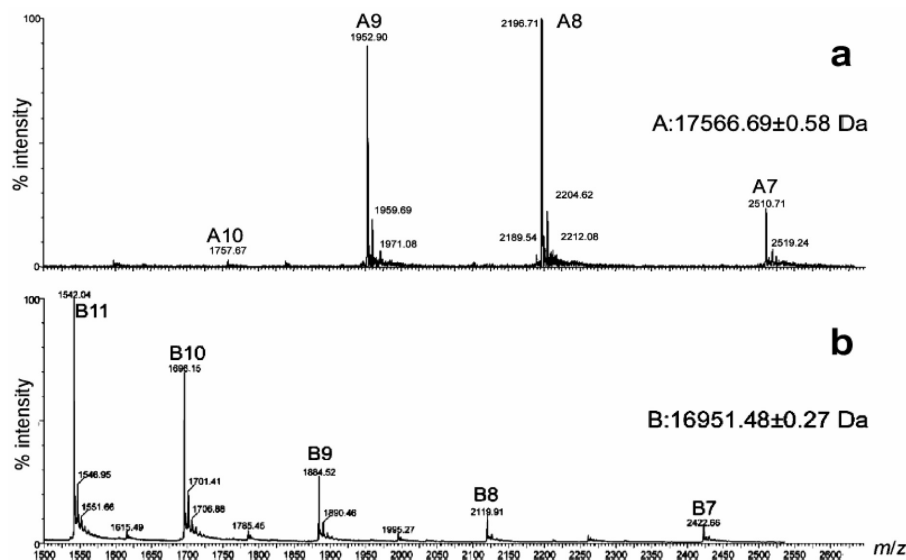


**Figure 5.** Comparison between HF FIFFF-ESI/TOFMS and RP HPLC-ESI/TOFMS of Mb. (a) Multicharged ion spectrum from HF FIFFF-ESI/TOFMS, (b) multicharged ion spectrum from RP HPLC-ESI/TOFMS. (Reprinted with permission from [44]; Copyright 2005 American Chemical Society.)

responding to the dimer and tetramer, respectively. Fractions of the Sigma uricase dimer and tetramer were collected and analyzed by MALDI-TOF-MS. Very interestingly, MALDI spectra showed the presence of uricase monomer in both fractions, which suggested that the MALDI process is breaking up the uricase oligomers. The enzyme activity analysis of the collected FFF fractions showed an increase in activity in the following order Rasburicase tetramer > Sigma uricase tetramer > Sigma uricase dimer. The lower specific activity of the Sigma uricase was partially attributed to the presence of the dimers.

The maintenance of the drug activity is a direct reflection of the survival of the native structures of the proteins after fractionation. FIFFF did not disrupt the noncovalent binding among subunits and between polypeptide chain and prosthetic group. This was clearly proved in the HF FIFFF analysis of apomyoglobin (Mb) with online detection by ESI-TOFMS [44]. Figure 5 is mass spectra of Mb separated by HF FIFFF and RP HPLC, respectively. The RP HPLC-ESI/TOFMS shows a higher protonation level than FIFFF-ESI/TOFMS, implying possible denaturation of the protein by RP HPLC. The molecular ion was 17 566.69 Da in the HF FIFFF-ESI/TOFMS and 16 951.48 Da in the RP HPLC-ESI/TOFMS. The difference between the two values was 615.21 Da, close to the nominal molar mass of the heme group (615.23 Da). HF FIFFF allowed elution of the intact protein with heme bound to Mb.

### 3.2 Supramolecular assemblies

A supramolecular assembly is a multicomponent system that is held together by noncovalent interactions, *e.g.*, hydrogen bonding, van der Waals forces, electrostatic

interactions, *etc.* These forces are weaker than covalent bonding making these assemblies sensitive to changes in their environments. Examples of FFF investigations of supramolecular assemblies are described in the following section. The protein aggregates discussed in the previous section could have also been included under this subheading.

#### 3.2.1 Ribosomes

Ribosomes are cellular organelles composed of protein and RNA and are the site for protein production. Extensive studies have been done on ribosomes using AsFIFFF [77–82]. Figure 6 shows an impressive fractionation of the 70S ribosome from the 30S and 50S subunits and tRNA and proteins. This degree of resolution made it possible to monitor ribosomal composition and tRNA levels and correlate them to cell growth and protein production levels [77, 81, 82]. The total analysis time of 16 min

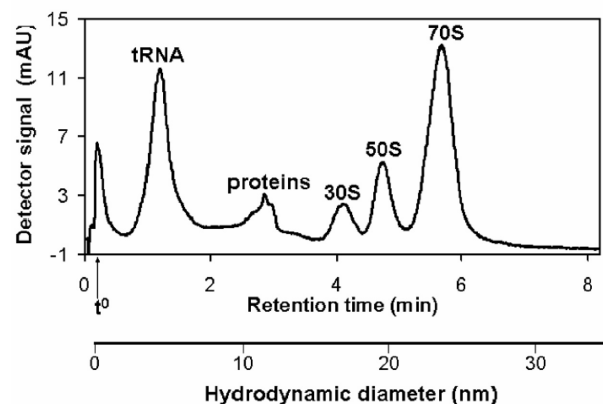


**Figure 6.** Asymmetric FIFFF analysis of a ribosomal sample taken at the exponential phase of cell growth. (Reprinted with permission from [78]; Copyright 2003 Elsevier.)

(6 min ribosome preparation, 8 min separation, 2 min wash) made this a viable technique for at-line optimization of cultivation conditions in bioreactors. Additional experiments turned up a previously unreported 100S particle that was believed to be a dimer of the 70S ribosomal particle [78].

### 3.2.2 Liposomes

Liposome size and size distributions were initially measured using FIFFF with UV detection [83]. The subsequent use of MALS-dRI as detectors allowed investigative studies of the effect of different buffers on the sizes of plain and encapsulated liposomes [84–87]. In addition, the shapes of the plain liposomes, hemoglobin-encapsulated liposomes, actin-encapsulated liposomes, and actin-hemoglobin-encapsulated liposomes were estimated by fitting different form factors to the light scattering intensities. The loaded liposomes transformed from spherical shape to disk-like shape as the concentration of the encapsulated actin increased. These results were consistent with atomic force microscopy measurements. Extensive screening was performed on the extrusion membrane pore sizes, actin concentrations, and hemoglobin concentrations to identify an appropriate condition to prepare liposome vesicles for use as blood substitutes.

### 3.2.3 Lipid: protein and lipid–DNA complexes

The “gentle” separation characteristic of FIFFF enabled a study of the interactions between cytochrome *c* and the lipid dimyristoylphosphatidylglycerol (DMPG) [88]. The hydrodynamic radius of cytochrome *c*-DMPG complexes at different pH were determined from the peak retention volumes in the fractograms using a calibration curve established from protein standards. The variation in sizes at different pH showed the effects of different modes of interactions (electrostatic or hydrophobic) on the sizes of the complexes.

Self-assembled cationic lipid–DNA gene carrier complexes of different charges were produced by combining different ratios of cationic lipid:DNA. The resulting heterogeneous mixtures containing lipids, DNA, liposomes, and lipid–DNA complexes were characterized with respect to size distributions and time [89]. FIFFF-MALS measurements showed that different size profiles were obtained for different lipid:DNA ratios (Fig. 7). In addition, a dynamic system was observed with smaller particles and aggregates forming as the mixture aged. Particle aggregation is of interest as it is one mechanism that reduces cell transfection efficiency. This work sets the stage for further studies involving nonviral vectors for gene delivery.

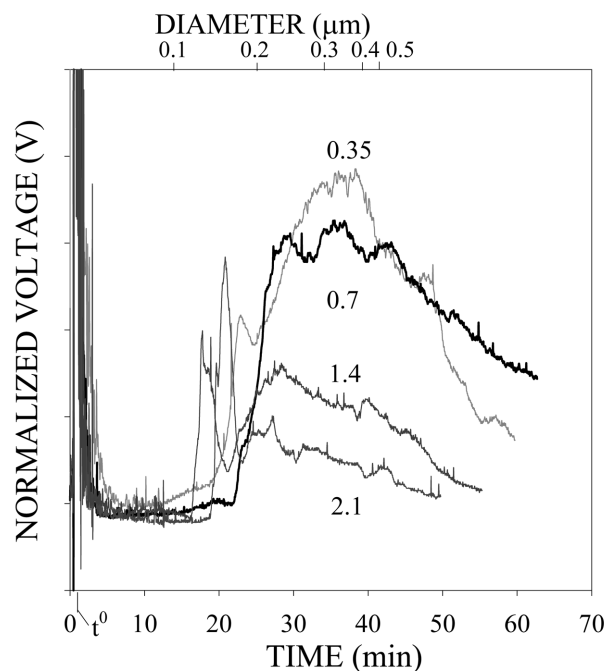


**Figure 7.** FIFFF of cationic lipid–DNA mixtures. Different lipid:DNA ratios resulted in different fractograms and size distributions. The y-axis represents the voltage output from the MALS detector and has been normalized so that the fractograms can be superimposed. (Reprinted with permission from [89]; Copyright 2001 American Chemical Society.)

### 3.2.4 Charged amphiphilic copolymer

The properties of the copolymer of poly(styrene-co-methyl methacrylate-co-maleic anhydride) grafted by PEG were studied by FIFFF [90–92]. The maleic anhydride on the backbone can react with water to form carboxylic acid and subsequently become charged under basic pH conditions. The hydrophobic group can associate in aqueous solution to form micelles; a tendency that is counterbalanced by electrostatic repulsion from the charges on the backbone. FIFFF was used to fractionate polymers prepared in the solution with different ionic strengths and pH. The sizes and populations of the micelles determined by FIFFF correlated well with the conditions of the aqueous solution. That is, an increase in salt concentration facilitated the formation of large size micelles because of “salt-out” effects and the maximum size occurred at a pH where the backbone was neutral. FIFFF yielded the expected size distributions, whereas the dynamic light scattering measurements showed a bias toward the large size population because of its stronger scattering intensity.

### 3.2.5 Poly(*N*-isopropylacrylamide)

Poly(*N*-isopropylacrylamide) (PNIPAM) is a thermo-responsive polymer, which undergoes a coil-to-globular

transition as the temperature is increased. The swollen chains collapse and aggregate at high temperature to form particles. Asymmetric FIFFF registered a dramatic size increase as the temperature increased and could thus be used to determine the critical transition temperature [93].

### 3.2.6 Microgels

The microgels, formed by *N*-vinylpyrrolidone, vinyl acetate, and diethylene glycol divinyl ether, were characterized by FIFFF-MALS [94]. The polymers showed molar masses from  $10^3$  to  $10^7$  Da. The polydispersity and molar mass of the microgels depended on the concentration of the monomers and crosslinker. Microgels are discussed further in a later section on organosoluble polymers using ThFFF.

### 3.3 Water-soluble synthetic polymers

FIFFF is the main FFF technique for studying water-soluble polymers. The effect of experimental factors, such as injected mass, ionic strength of the carrier liquid, and flow conditions, on the fractionation performance were investigated using neutral (polyacrylamide [95] and pullulan [96]), negatively charged (polysulfonate [95]), and positively charged (polyvinylpyridine [95]) polymer standards. It was observed that the elution times of polyelectrolytes were reduced when the sample load was increased. The degree of the decrease was mitigated when high ionic strength carrier liquids were used. These observations were attributed to the strong intermolecular electrostatic interactions inherent in polyelectrolyte systems. In contrast, neutral polymers such as pullulan exhibited increased retention times with increased sample loads. This may be due to hydrodynamic interactions between the polymer molecules [96].

A study of poly(ethylene oxide) (PEO) showed interesting results in that low molar mass PEO behaved differently in  $\text{Na}_2\text{SO}_4$  and  $\text{K}_2\text{SO}_4$  solutions [97]. Increases in sample loading had a slight effect on the retention time in  $\text{Na}_2\text{SO}_4$  solution but a remarkable decrease in  $\text{K}_2\text{SO}_4$  solution. PEO behaved like a polyelectrolyte because the potassium ion is tightly associated with the polymer.

The hyphenation of MALS with FIFFF provides direct determination of the molar mass distribution and size distribution of the polymers and makes conformation analysis possible. The suitability of FIFFF-MALS for polymer analysis was verified with polymer standards, such as polysulfonate [98], pullulan [99, 100], dextran [100, 101], polyacrylamide [102], and poly-diallyldimethylammonium chloride [101]. Since these initial studies with standards, FIFFF applications have been expanded considerably to investigate polymers of commercial importance.

### 3.4 Water-soluble natural polymers

The behavior of various types of polysaccharides in the FIFFF channel followed the same trend as those reported for neutral and charged water-soluble synthetic polymers [103]. The power of FIFFF-MALS was explored to characterize the high- and ultrahigh-molar mass components in these “natural” polymer samples.

#### 3.4.1 Starch

Starch consists of amylose (AMY) and amylopectin (AMP). The differentiating characteristics are that AMY is a linear chain and AMP is a branched chain and has a higher molar mass. The two components in corn starch, resolved by FIFFF-MALS, gave  $4.8 \times 10^5$  and  $4.5 \times 10^8$  g/mol as the MW of AMY and AMP, respectively [104]. The *rms*-MW plot indicated that the conformation of AMP, as expected, had a more compact structure than the lower molar mass components (AMY). Another study of AMP from waxy corn starch yielded an *rms* range of 250–1250 nm and molar masses from  $10^7$  to  $10^9$  g/mol [105]. In this case, the FFF separation occurred in the hyperlayer mode rather than the normal mode that we have described throughout this paper. The hyperlayer mode occurs when the diameter of the sample species is large relative to the diffusion distance. The separation is no longer based on differences in diffusion but rather on diameter. Larger particles elute first because their centers of mass protrude further from the accumulation wall and thus occupy faster velocity streamlines than the smaller particles. This FFF mode of operation occurs in the vicinity of 1  $\mu\text{m}$  and can be shifted to smaller or larger diameters depending on flow velocity and field strength [106]. The AMP *rms* of 1250 nm or 1.25  $\mu\text{m}$  fits the scenario for hyperlayer mode separation and the observed elution order was from large to small sizes. Similar to previous observations for synthetic water-soluble polymers, cationic potato AMP also showed a dependence of the elution on the ionic strength of the carrier liquid and the injected mass [107]. The fractograms exhibited tailing in low ionic strength carrier liquid which disappeared when a carrier liquid with 40 mM salt was used. The reproducibility of the fractionation was also improved. The  $M_w$  of the sample was  $5.2 \times 10^7$  g/mol with the *rms* range from 100 to 400 nm.

Modified starches, hydroxyethyl and hydroxypropyl starch, have also been analyzed [108]. Low sample recoveries (60–84%) were obtained due to loss of the low-molar mass components (radii <8 nm) through the membrane accumulation wall or to incomplete resolution from the void peak. Selective loss of the small size components resulted in overestimated MWs.

### 3.4.2 Cellulose derivatives

The initial FIFFF-MALS study of ethylhydroxyethyl cellulose (EHEC) uncovered the presence of an ultrahigh-molar mass component in the vicinity of  $10^8$  Da [109]. In a subsequent study involving EHEC samples from three different viscosity classes, programmed field strength FIFFF was employed [110]. By varying the crossflow rate from high to low, resolution could be maintained for the early eluting components and retention times decreased for the late eluting components. This strategy, which is similar to solvent strength programming in HPLC, is useful when separating highly polydisperse samples. Fractograms and molar masses of the three EHEC samples are shown in Fig. 8. Both of the lower viscosity class samples, EHEC I and II, exhibited two components that encompassed a broad molar mass distribution from  $10^4$  to  $10^9$  Da. Impressively, the high resolution analysis was completed in only 30 min. The slopes of  $\log rms$  versus  $\log M$  plots for both EHEC I and II revealed that the high-molar mass components ( $<10^7$  Da) had a random coil conformation, whereas the ultrahigh-molar mass components ( $>10^7$  Da) possessed a hyperbranched structure. The higher viscosity class EHEC III showed the presence of one peak and had lower polydispersity ( $5 \times 10^5$  to  $5 \times 10^7$  Da). A constant conformation corresponding to a collapsed coil was observed. In order to more closely examine the molar masses at the front and tail of the EHEC II peak, the sample load was increased 4.5 times to 450  $\mu\text{g}$ . It was noted that the increased sample load could cause a deterioration in separation resolution; which in turn, would explain the irregular behavior observed over a span of 2 min when the molar mass did not increase with time as previously observed in the lower sample loading experiment. This reinforces the importance of obtaining good resolution in the separation step preceding MALS measurements.

Methyl cellulose, methylhydroxyethyl cellulose, and carboxymethyl cellulose were also studied by FIFFF-MALS [111]. They all showed the presence of ultrahigh-molar mass components with compact structures.

### 3.4.3 Hyaluronan

Hyaluronan or hyaluronic acid is a long unbranched polysaccharide, composed of repeating dimeric units of glucuronic acid and *N*-acetyl glucosamine and has MWs ranging from a hundred thousand to several million Daltons. It is a naturally occurring macromolecule that lubricates joints, maintains the shape of eyeballs, and is a key component of connective tissue. It also forms the basis of cosmetic injectable fillers that temporarily remove the appearance of wrinkles. Interest in this polysaccharide stems from its many uses while the high MW and polydispersity make it a challenging analytical problem. The molar mass and *rms* of a series of hyaluronates

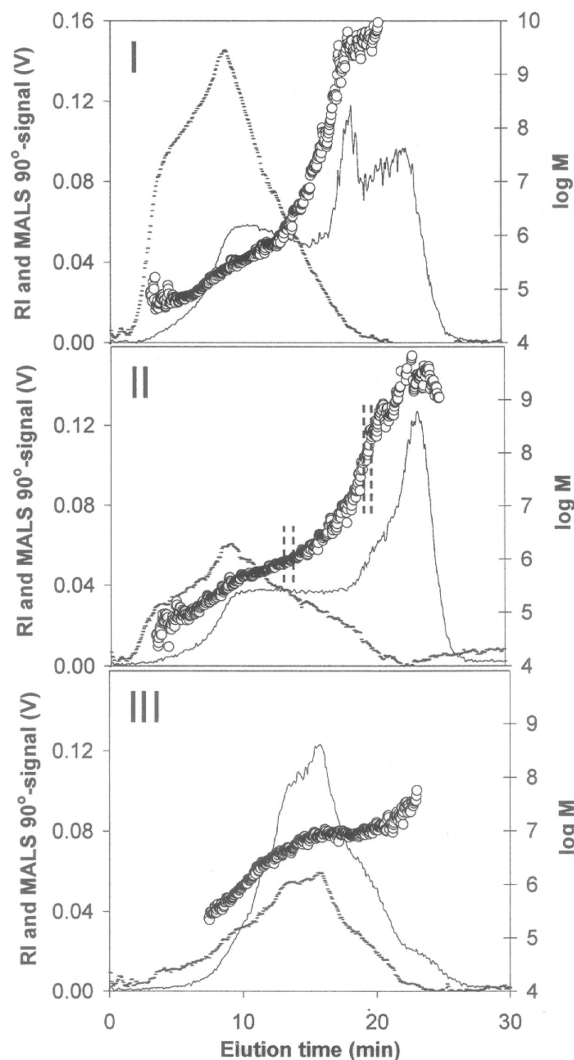


**Figure 8.** Asymmetric FIFFF-MALS of three different viscosity classes of ethylhydroxyethyl cellulose, EHEC I, II, and III. The solid lines represent the RI traces of the fractograms and the circles are molar masses. (Reprinted with permission from [110]; Copyright 2003 American Chemical Society.)

were measured by FIFFF-MALS and showed excellent agreement with results obtained from batch-mode light scattering measurements. This agreement suggested that the samples were not lost or degraded by the FFF process [112]. The effects of field programming and ionic strength of the carrier liquid were investigated [113]. A salt concentration of 0.1 M was necessary to obtain accurate results. The molar mass of the samples were from  $10^4$  to  $10^6$  g/mol and the *rms* radius were from  $<10$  to 200 nm.

### 3.4.4 Gum arabic

Gum arabic is composed of approximately 80% arabinogalactan (AG) and 20% AG-protein complex (AGP). AG,



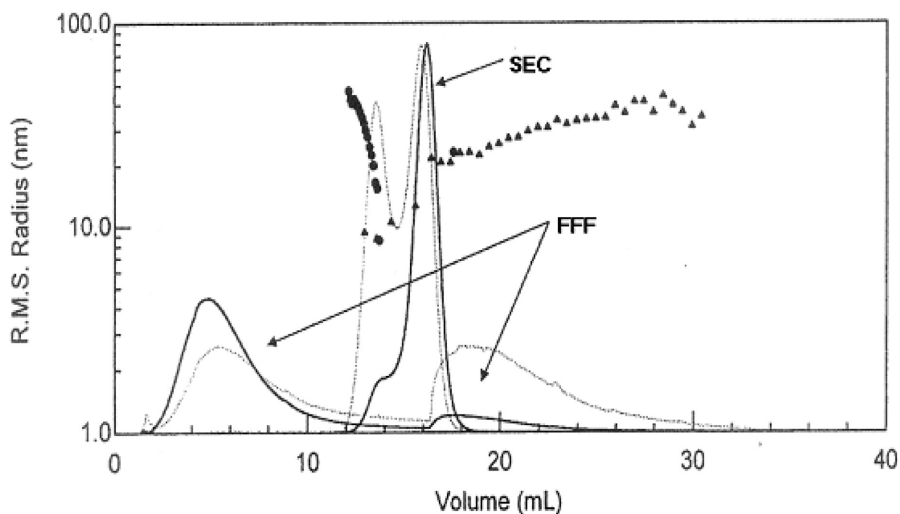


**Figure 9.** Comparison of the separation of gum Arabic by SEC (a) and FIFFF (b). Solid and dotted lines represent dRI and light scattering traces, respectively. Sphere and triangle symbols represent the *rms* radius. (Reprinted with permission from [114]; Copyright 2000 Elsevier.)

found in the heartwood of trees of the genus *Larix*, has a narrow MW distribution and is highly branched. The interest in this polysaccharide stems from its biocompatibility and its ability to inhibit cell adhesion and infection or inflammation. Figure 9 shows the separation results of gum arabic obtained using SEC and FIFFF [114]. The two components, AG and AGP, were completely resolved by FIFFF as shown by the two peaks at 5 and 18 mL, whereas SEC only showed partial separation with the peaks appearing at 13 and 16 mL. As a result, the molar mass of the AG component was overestimated while the AGP component was underestimated by SEC-MALS analysis. Correct measurement of the size of the AGP component was also not possible because of the interference by the AG peak. From FIFFF-MALS measurements, the MWs of AG and AGP were  $2.4 \times 10^5$  and  $2.6 \times 10^6$  g/mol, respectively. The size of AGP was 26 nm.

### 3.4.5 $\kappa$ -Carrageenan

$\kappa$ -Carrageenan is used as an emulsifier or thickener in food and can undergo coil-helix-rod-gel transitions as regulated by salt type or temperature [115, 116]. The helix conformation was formed through the binding of two polymer chains. Upon further aggregation, the helix evolved into a rod structure and eventually a 3-D gel network. A doubling of the molar mass recorded by FIFFF-MALS indicated the transition from coil to helix. The gradual transition from helix to rod was observed as an increase in molar mass from  $10^5$  to  $10^7$  g/mol.

## 3.5 Organosoluble polymers

### 3.5.1 Ultrahigh MW and microgels

In the FFF family, ThFFF is the technique used to characterize polymers in organic solvents. FIFFF channels compatible with organic solvents have only recently been introduced. ThFFF is complementary to SEC in that the

former is better suited for high-MW polymers and the latter for low-MW polymers. The crossover point, with respect to resolution, is  $\sim 10^5$  Da [117]. Like FIFFF, ThFFF can handle samples with extremely broad polydispersities.

The development of ThFFF has been slow in terms of application to industrial polymers. This may be due to (1) the incomplete understanding of the relationship between retention time and thermal diffusion and (2) the conventional approach of using a calibration curve constructed from polymer standards. The universal calibration methods were developed in an effort to enhance the analysis capability [118, 119]. Surprisingly, the studies of ThFFF hyphenated with MALS are scarce, in contrast to the explosion of FIFFF-MALS investigations.

Rubber has been the focus of a series of papers [120–122]. ThFFF-MALS analysis of a styrene-butadiene rubber showed an ultrahigh molar mass component between  $10^7$  and  $10^8$  g/mol [120]. This component, which accounted for 10% of the sample, was not detected in SEC-MALS analysis. An important conclusion of these studies was that the filtration step performed prior to SEC separation removed a significant portion of the sample and led to erroneously low-MW averages.

Recently, ThFFF-MALS was applied to samples of poly(vinyl acetate) that had been prepared by emulsion polymerization. The polymer contained nanogels and microgels. Figure 10 shows the elution profiles and the measured molar mass of an unfiltered and a 0.5  $\mu\text{m}$  pore-size filtered sample. At early elution volumes (<2 mL), a strong scattering signal was observed for the unfiltered sample. The decrease in molar mass in the first 2 mL suggested that the large size polymer aggregates were eluting in the hyperlayer mode. The fractionation proceeded in the normal mode after 2 mL as indicated by the increase in MW. The unfiltered sample showed at least

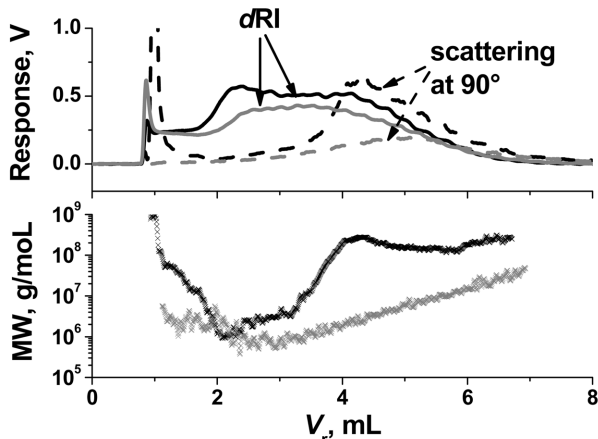


**Figure 10.** ThFFF-MALS/dRI analysis of poly(vinyl acetate). (a) Light scattering (90°) and dRI fractograms, (b) molar mass. Gray traces correspond to the 0.5 μm pore-size filtered sample and black traces correspond to the unfiltered sample. Solid and dashed lines represent dRI and light scattering fractograms, respectively. Cross symbols represent molar mass. Conditions:  $\Delta T = \Delta T_0(t_1 - t_a)/(t_1 - t_a)^2$ ;  $\Delta T_0 = 55^\circ\text{C}$ ,  $t_1 = 15\text{ min}$ ,  $t_a = -1\text{ min}$ ; flow rate, 0.1 mL/min; carrier liquid, ACN; injection volume, 20 μL.

one order magnitude higher molar mass than the filtered sample. Additional experiments done using binary solvents resulted in complete suspension of the entire sample. This indicated that the nanogels/microgels consisted of associated polymer chains rather than cross-linked polymers. These results demonstrate the advantage of ThFFF in analysis of ultrahigh molar mass polymers and the importance of analyzing an unfiltered sample.

### 3.5.2 Composition separations

ThFFF has proven to be a useful method for measuring  $D_T$  for different polymer–solvent combinations. This has enabled certain commonalities to surface and new thermal diffusion models [56, 123] to be introduced. One finding common among  $D_T$  studies is that polymer–solvent interactions are important. Consequently, retention times can be significantly shifted by changing the separation solvent [53, 124, 125]. Figure 11 is a plot of  $D_T$  versus polystyrene MW [126]. This plot shows that  $D_T$  is independent of MW and dependent on the solvent. Figure 11 also suggests that polymers possessing the same MW but different compositions can be separated. For example, polyisoprene and polymethylmethacrylate of the same MW will have more than two times difference in retention time if the ThFFF separation was performed in toluene.

ThFFF separations by composition have been demonstrated with mixtures of polystyrene and poly(2-vinylpyridine) [60]. This allowed each polymer to be analyzed by MALDI-TOF-MS using different optimum conditions that were tailored for each polymer. Selective MALDI ionization and detection have been reported for polydisperse (polydispersity index >1.2) polymers and polymer mixtures [63]. The use of ThFFF to produce more homogeneous fractions prior to MALDI is an important step in obtaining accurate MALDI measurements. MALDI-MS, on the other hand, provides MW information and confirms the identity of the polymer thereby eliminating the need for ThFFF standards [60].

ThFFF has also been coupled with SEC in a 2-D separation involving a mixture of polystyrene, polybutadiene, and

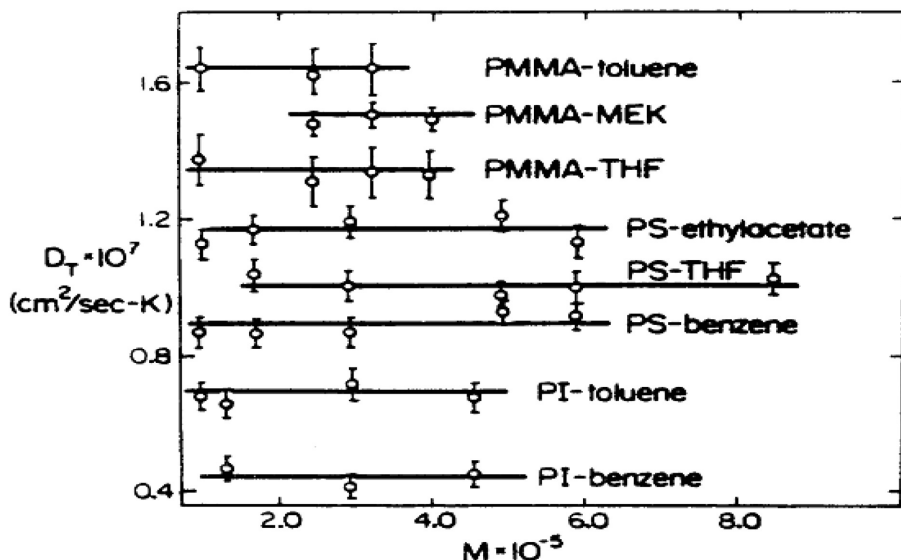


**Figure 11.** Relationship between thermal diffusion coefficient  $D_T$  and molecular weight (MW) for different polymer–solvent combinations. Polymethylmethacrylate (PMMA), polystyrene (PS), polyisoprene (PI and THF, methylethylketone (MEK). (Reprinted with permission from [126]; Copyright 1989 John Wiley & Sons.)

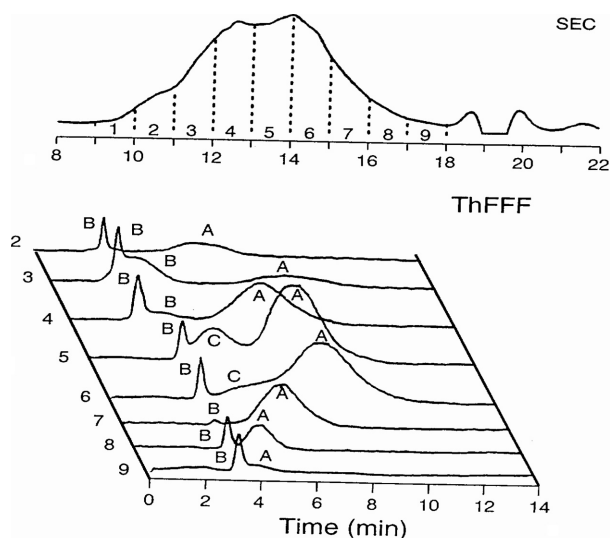


**Figure 12.** 2-D separation of a mixture composed of polystyrene (A), polybutadiene (B), and polytetrahydrofuran (C). Fractions containing equal size polymers were collected at the SEC outlet and injected into ThFFF for a composition-based separation. (Reprinted with permission from [61]; Copyright 1995 Elsevier.)

polyTHF [61]. Same-size fractions were obtained using SEC. These fractions were then injected into a ThFFF channel and separated by composition as shown in Fig. 12. As more polymer mixtures are used to obtain specific materials properties, multidimensional separations such as that shown here may become more common place.

## 4 Conclusions

Forty years after the first publication, flow and ThFFF are emerging as the separation methods for high- and ultra-high-MW macromolecules, nanometer- to micrometer-size sample species, and complex heterogeneous sample mixtures. These types of materials are difficult to separate by other methods. FFF is a gentle separation technique that has been shown in many instances to retain enzyme activity and cell viability. Elution profiles can be used to monitor changes in size distributions of dynamic systems such as supramolecular assemblies. Fractions can be collected upon elution from the FFF channel and tested for infectivity and transfection efficiency. Combining FFF with other techniques such as light scattering and MS yields additional “localized” information about conformation and identity of the eluted fraction.

With these characteristics and capabilities, why has FFF not experienced explosive growth and become a mainstream analytical technique? Part of this is due to timing. FFF was introduced at a time when research interests focused primarily on molecule-size entities and the terms nanoscience and nanotechnology were unknown.

Another explanation may be FFF’s versatility. There are many more forms of FFF (sedimentation, electrical, dielectrophoretic, magnetic, and acoustic) than the two discussed in this review. This versatility may be as much a hindrance as an asset because determining the best FFF technique for a particular application requires sufficient knowledge about the other FFF techniques. This will change as the number of publications in key application areas increase. Finally, there has been limited availability of commercial instrumentation. However, in the last 3 years, the number of companies offering FFF systems has increased from one to four. These companies offer light scattering detector options which will provide an independent measure of MW and size for comparison with values calculated using retention volumes and FFF theory and compensates for nonidealities encountered in the FFF process. With increased competition, this should bode well for those considering research and applications involving FFF.

*We gratefully acknowledge support from the National Science Foundation (CHE 0515521) and ICI.*

## 5 References

- [1] Marston, F. A. O., Lowe, P. A., Doel, M. T., Schoemaker, J. M. *et al.*, *BioTechnology* 1984, 2, 800–804.
- [2] Schoemaker, J. M., Brasnett, A. H., Marston, F. A. O., *EMBO J.* 1985, 4, 775–780.
- [3] Uversky, V. N., Fink, A. L., *BBA-Proteins Proteomics* 2004, 1698, 131–153.
- [4] Hansen, F. K., *ACS Symp. Ser.* 1991, 472, 169–183.
- [5] Desai, M. J., Armstrong, D. W., *Microbiol. Mol. Biol. Rev.* 2003, 67, 38–51.
- [6] Dos Ramos, J. G., *ACS Symp. Ser.* 2004, 881, 138–150.
- [7] Giddings, J. C., *Science* 1993, 260, 1456–1465.
- [8] Giddings, J. C., *Anal. Chem.* 1995, 67, A592–A598.
- [9] Giddings, J. C., *Sep. Sci.* 1966, 1, 123–125.
- [10] Chen, B. L., Selegue, J. P., *Anal. Chem.* 2002, 74, 4774–4780.
- [11] Liu, J., Rinzler, A. G., Dai, H. J., Hafner, J. H. *et al.*, *Science* 1998, 280, 1253–1256.
- [12] Guglielmi, L., Battu, S., Le Bert, M., Faucher, J. L. *et al.*, *Anal. Chem.* 2004, 76, 1580–1585.
- [13] Gascoyne, P. R. C., Vykoukal, J. V., *Proc. IEEE* 2004, 92, 22–42.
- [14] Lee, H., Williams, S. K. R., Wahl, K. L., Valentine, N. B., *Anal. Chem.* 2003, 75, 2746–2752.
- [15] Reschiglian, P., Zattoni, A., Roda, B., Casolari, S. *et al.*, *Anal. Chem.* 2002, 74, 4895–4904.
- [16] Reschiglian, P., Zattoni, A., Cinque, L., Roda, B. *et al.*, *Anal. Chem.* 2004, 76, 2103–2111.
- [17] Saenton, S., Lee, H., Gao, Y. S., Ranville, J. F., Williams, S. K. R., *Sep. Sci. Technol.* 2000, 35, 1761–1775.
- [18] Gallet, S., Metreau, J. M., Loiseau, P. M., Bories, C., Car-dot, P. J. P., *J. Microcolumn Sep.* 1997, 9, 469–477.

- [19] Gascoyne, P., Mahidol, C., Ruchirawat, M., Satayavivad, J. *et al.*, *Lab Chip* 2002, 2, 70–75.
- [20] Gascoyne, P., Satayavivad, J., Ruchirawat, M., *Acta Trop.* 2004, 89, 357–369.
- [21] Carro, S., Herrera-Ordonez, J., *Macromol. Rapid Commun.* 2006, 27, 274–278.
- [22] Van Quynh, A., Blanchart, P., Battu, S., Cledat, D., Cardot, P., *J. Chromatogr. A* 2006, 1108, 90–98.
- [23] Leger, D. Y., Liagre, B., Cardot, P. J. P., Beneytout, J. L., Battu, S., *Anal. Biochem.* 2004, 335, 267–278.
- [24] Beckett, R., Ho, J., Jiang, Y., Giddings, J. C., *Langmuir* 1991, 7, 2040–2047.
- [25] Fromell, K., Andersson, M., Elihn, K., Caldwell, K. D., *Colloids Surf. B* 2005, 46, 84–91.
- [26] Hartmann, R. L., Williams, S. K. R., *J. Memb. Sci.* 2002, 209, 93–106.
- [27] Williams, P. S., Koch, T., Giddings, J. C., *Chem. Eng. Commun.* 1992, 111, 121–147.
- [28] Schimpf, M. E., Caldwell, K., Giddings, J. C. (Eds), *Field-Flow Fractionation Handbook*, John Wiley & Sons, New York 2000.
- [29] Janca, J., *Field-Flow Fractionation*, Marcel Dekker, New York 1988.
- [30] Schimpf, M. E., *J. Liq. Chromatogr. Related Technol.* 2002, 25, 2101–2134.
- [31] Williams, S. K. R., Benincasa, M. A., in: Meyers, R. A. (Eds), *Encyclopedia of Analytical Chemistry*, John Wiley & Sons, Chichester 2000, pp. 7582–7608.
- [32] Kassalainien, G. E., Williams, S. K. R., in: Cazes, J. (Eds), *Encyclopedia of Chromatography*, Marcel Dekker, New York 2002, pp. 680–683.
- [33] Fraunhofer, W., Winter, G., *Eur. J. Pharm. Biopharm.* 2004, 58, 369–383.
- [34] Reschiglian, P., Zattoni, A., Roda, B., Michelini, E., Roda, A., *Trends Biotechnol.* 2005, 23, 475–483.
- [35] Barman, B. N., Giddings, J. C., *Langmuir* 1992, 8, 51–58.
- [36] Caldwell, K. D., Giddings, J. C., Myers, M. N., Kesner, L. F., *Science* 1972, 176, 296.
- [37] Lao, A. I. K., Hsing, I. M., *Lab Chip* 2005, 5, 687–690.
- [38] Davis, J. M., Fan, F. R. F., Bard, A. J., *Anal. Chem.* 1987, 59, 1339–1348.
- [39] Ratanathanawongs, S. K., Lee, I., Giddings, J. C., *ACS Symp. Ser.* 1991, 472, 229–246.
- [40] Wahlund, K. G., Giddings, J. C., *Anal. Chem.* 1987, 59, 1332–1339.
- [41] Litzen, A., Wahlund, K. G., *J. Chromatogr.* 1989, 476, 413–421.
- [42] Wahlund, K. G., Litzen, A., *J. Chromatogr.* 1989, 461, 73–87.
- [43] Lee, H. L., Reis, J. F. G., Dohner, J., Lightfoot, E. N., *AIChE J.* 1974, 20, 776–784.
- [44] Reschiglian, P., Zattoni, A., Roda, B., Cinque, L. *et al.*, *Anal. Chem.* 2005, 77, 47–56.
- [45] Lee, W. J., Min, B. R., Moon, M. H., *Anal. Chem.* 1999, 71, 3446–3452.
- [46] Zhu, R. H., Frankema, W., Huo, Y. L., Kok, W. T., *Anal. Chem.* 2005, 77, 4581–4586.
- [47] Giddings, J. C., *Anal. Chem.* 1990, 62, 2306–2312.
- [48] Giddings, J. C., Caldwell, K., Kesner, L. F., in: Cooper, A. R. (Eds), *Determination of Molecular Weight*, John Wiley & Sons, New York 1989, pp. 337–372.
- [49] Wyatt, P. J., *Anal. Chim. Acta* 1993, 272, 1–40.
- [50] Andersson, M., Wittgren, B., Wahlund, K. G., *Anal. Chem.* 2003, 75, 4279–4291.
- [51] Liu, G., Giddings, J. C., *Anal. Chem.* 1991, 63, 296–299.
- [52] Shiundu, P. M., Williams, S. K. R., *ACS Symp. Ser.* 2004, 881, 185–198.
- [53] Kassalainien, G. E., Williams, S. K. R., *J. Chromatogr. A* 2003, 988, 285–295.
- [54] Nguyen, M., Beckett, R., *Anal. Chem.* 2004, 76, 2382–2386.
- [55] Rauch, J., Kohler, W., *Macromolecules* 2005, 38, 3571–3573.
- [56] Schimpf, M. E., Semenov, S. N., *J. Phys. Chem. B* 2000, 104, 9935–9942.
- [57] Wiegand, S., *J. Phys. Condens. Matter* 2004, 16, R357–R379.
- [58] Semenov, S. N., Schimpf, M. E., *Phys. Rev. E* 2005, 72, 041202C1–9.
- [59] Schimpf, M. E., Wheeler, L. M., Romeo, P. F., *ACS Symp. Ser.* 1993, 521, 63–76.
- [60] Kassalainien, G. E., Williams, S. K. R., *Anal. Chem.* 2003, 75, 1887–1894.
- [61] van Asten, A. C., van Dam, R. J., Kok, W. T., Tijssen, R., Poppe, H., *J. Chromatogr. A* 1995, 703, 245–263.
- [62] Jeon, S. J., Schimpf, M. E., Nyborg, A., *Anal. Chem.* 1997, 69, 3442–3450.
- [63] Byrd, H. C. M., McEwen, C. N., *Anal. Chem.* 2000, 72, 4568–4576.
- [64] Edwards, T. L., Gale, B. K., Frazier, A. B., *Anal. Chem.* 2002, 74, 1211–1216.
- [65] Janca, J., *J. Liq. Chromatogr. Rel. Technol.* 2002, 25, 2173–2191.
- [66] Janca, J., *Anal. Chim. Acta* 2005, 540, 187–196.
- [67] Janca, J., *Int. J. Polym. Anal. Charact.* 2006, 11, 57–70.
- [68] Giddings, J. C., Yang, F. J., Myers, M. N., *Anal. Biochem.* 1977, 81, 395–407.
- [69] Park, I., Paeng, K. J., Yoon, Y., Song, J. H., Moon, M. H., *J. Chromatogr. B* 2002, 780, 415–422.
- [70] Pauck, T., Colfen, H., *Anal. Chem.* 1998, 70, 3886–3891.
- [71] Liu, M. K., Giddings, J. C., *Macromolecules* 1993, 26, 3576–3588.
- [72] Stevenson, S. G., Preston, K. R., *J. Cereal Sci.* 1996, 23, 121–131.
- [73] Stevenson, S. G., Ueno, T., Preston, K. R., *Anal. Chem.* 1999, 71, 8–14.
- [74] Stevenson, S. G., You, S., Izydorczyk, M. S., Preston, K. R., *J. Liq. Chromatogr. Relat. Technol.* 2003, 26, 2771–2781.
- [75] Silveira, J. R., Raymond, G. J., Hughson, A. G., Race, R. E. *et al.*, *Nature* 2005, 437, 257–261.
- [76] Roda, A., Parisi, D., Guardigli, M., Zattoni, A., Reschiglian, P., *Anal. Chem.* 2006, 78, 1085–1092.
- [77] Andersson, C. I. J., Arfvidsson, C., Kallio, P. T., Wahlund, K. G., Bulow, L., *Biotechnol. Lett.* 2003, 25, 1499–1504.

- [78] Arfvidsson, C., Wahlund, K. G., *Anal. Biochem.* 2003, 313, 76–85.
- [79] Nilsson, M., Birnbaum, S., Wahlund, K. G., *J. Biochem. Biophys. Meth.* 1996, 33, 9–23.
- [80] Nilsson, M., Bulow, L., Wahlund, K. G., *Biotechnol. Bioeng.* 1997, 54, 461–467.
- [81] Nilsson, M., Wahlund, K. G., Bulow, L., *Biotechnol. Techniques* 1998, 12, 477–480.
- [82] Nilsson, M., Kallio, P. T., Bailey, J. E., Bulow, L., Wahlund, K. G., *Biotechnol. Prog.* 1999, 15, 158–163.
- [83] Moon, M. H., Giddings, J. C., *J. Pharm. Biomed. Anal.* 1993, 11, 911–920.
- [84] Arifin, D. R., Palmer, A. F., *Biotechnol. Prog.* 2003, 19, 1798–1811.
- [85] Arifin, D. R., Palmer, A. F., *Artif. Cell. Blood Substit. Bio.* 2005, 33, 113–136.
- [86] Li, S., Palmer, A. F., *Langmuir* 2004, 20, 4629–4639.
- [87] Li, S. L., Nickels, J., Palmer, A. F., *Biomaterials* 2005, 26, 3759–3769.
- [88] Yohannes, G., Wiedmer, S. K., Tuominen, E. K. J., Kinnunen, P. K. J., Riekkola, M. L., *Anal. Bioanal. Chem.* 2004, 380, 757–766.
- [89] Lee, H., Williams, S. K. R., Allison, S. D., Anchordoquy, T. J., *Anal. Chem.* 2001, 73, 837–843.
- [90] Derand, H., Wesslen, B., Wittgren, B., Wahlund, K. G., *Macromolecules* 1996, 29, 8770–8775.
- [91] Wittgren, B., Wahlund, K. G., Derand, H., Wesslen, B., *Macromolecules* 1996, 29, 268–276.
- [92] Wittgren, B., Wahlund, K. G., Derand, H., Wesslen, B., *Langmuir* 1996, 12, 5999–6005.
- [93] Yohannes, G., Shan, J., Jussila, M., Nuopponen, M., Tenhu, H., Riekkola, M. L., *J. Sep. Sci.* 2005, 28, 435–442.
- [94] de Groot, J. H., Zurutuza, A., Moran, C. R., Graham, N. B. *et al.*, *Colloid Polym. Sci.* 2001, 279, 1219–1224.
- [95] Benincasa, M. A., Giddings, J. C., *J. Microcolumn Sep.* 1997, 9, 479–495.
- [96] Benincasa, M. A., Delle Fratte, C., *J. Chromatogr. A* 2004, 1046, 175–184.
- [97] Benincasa, M. A., Caldwell, K. D., *J. Chromatogr. A* 2001, 925, 159–169.
- [98] Thielking, H., Kulicke, W. M., *Anal. Chem.* 1996, 68, 1169–1173.
- [99] Adolphi, U., Kulicke, W. M., *Polymer* 1997, 38, 1513–1519.
- [100] Wittgren, B., Wahlund, K. G., *J. Chromatogr. A* 1997, 760, 205–218.
- [101] Thielking, H., Kulicke, W. M., *J. Microcolumn Sep.* 1998, 10, 51–56.
- [102] Hecker, R., Fawell, P. D., Jefferson, A., Farrow, J. B., *J. Chromatogr. A* 1999, 837, 139–151.
- [103] Benincasa, M. A., Cartoni, G., Delle Fratte, C., *J. Chromatogr. A* 2002, 967, 219–234.
- [104] Roger, P., Baud, B., Colonna, P., *J. Chromatogr. A* 2001, 917, 179–185.
- [105] van Bruijnsvoort, M., Wahlund, K. G., Nilsson, G., Kok, W. T., *J. Chromatogr. A* 2001, 925, 171–182.
- [106] Jensen, K. D., Williams, S. K. R., Giddings, J. C., *J. Chromatogr. A* 1996, 746, 137–145.
- [107] Lee, S., Nilsson, P. O., Nilsson, G. S., Wahlund, K. G., *J. Chromatogr. A* 2003, 1011, 111–123.
- [108] Wittgren, B., Wahlund, K. G., Andersson, M., Arfvidsson, C., *Int. J. Polym. Anal. Charact.* 2002, 7, 19–40.
- [109] Andersson, M., Wittgren, B., Wahlund, K. G., *Anal. Chem.* 2001, 73, 4852–4861.
- [110] Andersson, M., Wittgren, B., Schagerlof, H., Momcilovic, D., Wahlund, K. G., *Biomacromolecules* 2004, 5, 97–105.
- [111] Kulicke, W. M., Clasen, C., Lohman, C., *Macromol. Symposia* 2005, 223, 151–174.
- [112] Takahashi, R., Al Assaf, S., Williams, P. A., Kubota, K. *et al.*, *Biomacromolecules* 2003, 4, 404–409.
- [113] Lee, H., Kim, H., Moon, M. H., *J. Chromatogr. A* 2005, 1089, 203–210.
- [114] Picton, L., Bataille, I., Muller, G., *Carbohydr. Polym.* 2000, 42, 23–31.
- [115] Wittgren, B., Borgstrom, J., Piculell, L., Wahlund, K. G., *Biopolymers* 1998, 45, 85–96.
- [116] Viebke, C., Williams, P. A., *Food Hydrocolloids* 2000, 14, 265–270.
- [117] Kirkland, J. J., Yau, W. W., *Macromolecules* 1985, 18, 2305–2311.
- [118] Pasti, L., Melucci, D., Contado, C., Dondi, F., Mingozi, I., *J. Sep. Sci.* 2002, 25, 691–702.
- [119] Pasti, L., Bedani, F., Contado, C., Mingozi, I., Dondi, F., *Anal. Chem.* 2004, 76, 6665–6680.
- [120] Sibbald, M., Lewandowski, L., Mallamaci, M., Johnson, E., *Macromol. Symp.* 2000, 155, 213–228.
- [121] Lee, S., Eum, C. H., Plepys, A. R., *Bull. Kor. Chem. Soc.* 2000, 21, 69–74.
- [122] Kim, W. S., Eum, C. H., Molnar, A., Yu, J. S., Lee, S., *Analytst* 2006, 131, 429–433.
- [123] Mes, E. P. C., Kok, W. T., Tijssen, R., *Int. J. Polym. Anal. Charact.* 2003, 8, 133–153.
- [124] Sisson, R. M., Giddings, J. C., *Anal. Chem.* 1994, 66, 4043–4053.
- [125] Rue, C. A., Schimpf, M. E., *Anal. Chem.* 1994, 66, 4054–4062.
- [126] Schimpf, M. E., Giddings, J. C., *J. Polym. Sci. B Polym. Phys.* 1989, 27, 1317–1332.